Massless monopoles and the moduli space approximation

Xingang Chen,* Huidong Guo,† and Erick J. Weinberg‡
Department of Physics, Columbia University, New York, New York 10027
(Received 7 August 2001; published 26 November 2001)

We investigate the applicability of the moduli space approximation in theories with unbroken non-Abelian gauge symmetries. Such theories have massless magnetic monopoles that are manifested at the classical level as clouds of non-Abelian field surrounding one or more massive monopoles. Using an SO(5) example with one massive and one massless monopole, we compare the predictions of the moduli space approximation with the results of a numerical solution of the full field equations. We find that the two diverge when the cloud velocity becomes of order unity. After this time the cloud profile approximates a spherical wavefront moving at the speed of light. In the region well behind this wavefront the moduli space approximation continues to give a good approximation to the fields. We therefore expect it to provide a good description of the motion of the massive monopoles and of the transfer of energy between the massive and massless monopoles.

DOI: 10.1103/PhysRevD.64.125004 PACS number(s): 11.27.+d, 14.80.Hv

I. INTRODUCTION

The moduli space approximation (MSA) [1] is a useful tool for studying the low-energy dynamics of Bogomolny-Prasad-Sommerfield (BPS) magnetic monopoles [2,3] and other systems that allow families of static multisoliton solutions. In this approximation the full field dynamics is replaced by that of the small number of collective coordinates that span the moduli space of static solutions. This neglects possible distortions of the inner structure of the solitons, and thus effectively treats them as point particles. The approximation is expected to be valid when the soliton velocity $v \ll 1$, with corrections suppressed by powers of v. This suggests that it might break down in certain gauge theories where, as we describe below, some BPS monopoles are effectively transformed into massless particles [4]. Indeed, a study by two of us [5] of monopole scattering in one such theory encountered anomalies that suggest a breakdown of the MSA. In this paper we describe some analytic and numerical calculations that shed light on this issue.

The MSA can be motivated by recalling some features of the spectrum of small oscillations about a multisoliton solution. First, there are a number of zero-frequency modes that are handled by the introduction of the collective coordinates. Next, for each elementary field of mass m_i in the theory there is a continuum spectrum beginning with minimum energy $E=m_i$. Finally, there may be some discrete nonzero eigenvalues. The last two components of the spectrum correspond to scattering states and bound states, respectively, of the massive quanta in the presence of the solitons. If the soliton kinetic energies are much smaller than the m_i, excitation of these modes should be suppressed. In the MSA one assumes that this suppression is complete and takes the collective coordinates to be the only dynamical degrees of freedom. If, as is the case for BPS solutions, the static energy is independent of the collective coordinates, the effective Lagrangian for the collective coordinates has only kinetic energy terms. These define a metric on the moduli space, and the classical evolution of the system is equivalent to geodesic motion with respect to this metric.

The energetic arguments underlying the MSA apply fairly straightforwardly to theories with only massive fields. However, when massless fields are present, as is the case in theories with magnetic monopoles, radiation of low-energy quanta is always energetically possible. To justify the MSA, one must show that this radiation is suppressed at low monopole velocities. The simplest case to consider is that of an SU(2) theory broken to U(1), with gauge coupling e, a massive vector boson of mass m, and a monopole mass $M \sim 4\pi m/e^2$. The problem of radiation in this theory was first addressed by Manton and Samols [6]. For well-separated monopoles the amount of U(1) ''electromagnetic'' radiation[1] can be estimated by treating the monopoles as point magnetic charges moving along the trajectories specified by the MSA. Standard electromagnetic techniques show that the total dipole radiation is of order Mv^3, while higher multipoles are suppressed by additional powers of v. (For the case of two monopoles, the dipole moment vanishes identically, so the quadrupole term dominates and the total radiation is of order Mv^5.) These arguments break down if the monopoles approach closely enough that their cores actually collide and overlap. However, since the core radius is of order m^{-1}, the dominant effect should only be on modes of wavelength $\lesssim m^{-1}$, with quanta of energy $\gtrsim m$, and these can be neglected because of energetic considerations. These somewhat heuristic arguments have been placed on a more rigorous footing by Stuart [7].

Now consider BPS monopoles in a theory with a gauge group G of rank $k>1$. For generic vacuum expectation values of the adjoint Higgs field the symmetry is broken to the maximum Abelian subgroup $U(1)^k$. There are then k distinct topological charges. Associated with each is a fundamental monopole [8], carrying one unit of that charge, that can be

*Email address: xgchen@phys.columbia.edu
†Email address: guohd@phys.columbia.edu
‡Email address: ejw@phys.columbia.edu

[1]There is also radiation of the massless scalar field, which can be handled by similar methods.

realized as an embedding of the SU(2) unit monopole in the SU(2) subgroup defined by one of the simple roots of G. All higher-charged BPS solutions can be understood as multimonopole solutions containing appropriate numbers of the various species of fundamental monopoles. As long as the fundamental monopoles all remain massive, the arguments used to justify the MSA in the SU(2) theory can be readily extended to this more general case.

The situation is more complex if the Higgs field is such that the unbroken gauge group has a non-Abelian component. When this happens, the masses of some of the fundamental monopoles vanish. These massless monopoles, which can be viewed as the counterparts of the massless non-Abelian gauge bosons, cannot be realized as isolated classical solutions. Instead, they are manifested in classical multimonopole solutions as ''clouds'' surrounding one or more massive monopoles [4]. Both Abelian and non-Abelian magnetic fields are present within the cloud region, but outside the cloud the non-Abelian components are suppressed by powers of r relative to the Abelian Coulomb magnetic fields. For static solutions the energy is independent of the size of the cloud.

One might well expect to encounter some difficulties with the MSA in this case. First, the presence of massless non-Abelian gauge fields gives more possibilities for low-energy radiation. Second, the charged fields that are the source for this radiation are not confined to a core region of size $\sim m^{-1}$, as in the case of Abelian breaking, but are instead present throughout the cloud region, which can be arbitrarily large. Finally, the vanishing mass of some of the monopoles seems inconsistent with the low-velocity regime that is required for the MSA.

This last point needs some elaboration. Because the massless monopoles do not have well-defined positions, their velocities are also not well defined. However, there is an associated quantity with dimensions of velocity, namely the rate of expansion of the cloud region. This need not be unity, as an ordinary massless-particle velocity would be. On the other hand, even if this ''cloud velocity'' is initially small, there is no guarantee that it will remain small, or even bounded. For example, in Ref. [5], the MSA was used to study solutions containing two massive monopoles and a massless cloud in an SU(N) theory. It was found that the massive monopoles tend toward a constant velocity at large times, but that the cloud size varies roughly as kt^2, where k is proportional to the kinetic energy associated with the cloud. Thus, no matter how small this energy, the MSA predicts that the cloud eventually expands faster than the speed of light.

The prediction of such superluminal expansion in a relativistic field theory suggests a breakdown of the MSA. In principle, one could test this by solving the full time-dependent field equations and comparing with the MSA predictions. For arbitrary configurations of the SU(N) monopoles this would be a fairly difficult undertaking. We therefore focus instead on another example that shares many of the essential features of the SU(N) solutions but that is analytically more tractable.

The example [9] we consider occurs in a theory with an SO(5) gauge symmetry broken to SU(2)$\times$U(1) by an adjoint Higgs field. There are two species of fundamental monopoles, one massive and one massless. The static BPS solutions containing one of each are all spherically symmetric and contain a massive core of fixed radius surrounded by a cloud of arbitrary radius a. Suppressing the dependence on the other collective coordinates, we denote the corresponding fields by $A_\mu^{\rm BPS}(\mathbf{r},a)$ and $\Phi^{\rm BPS}(\mathbf{r},a)$.

If we work in the center-of-mass frame and restrict ourselves to solutions with vanishing SU(2) and U(1) electric charges, the cloud radius is the only time-dependent collective coordinate. Solving the Euler-Lagrange equation following from the moduli space Lagrangian gives a solution $a_{\rm MSA}(t)$. The MSA consists of assuming that the time-dependence of the fields arises solely from that of a, and that the latter is given by $a_{\rm MSA}(t)$. Explicitly,

$$A_\mu^{\rm MSA}(\mathbf{r},t)=A_\mu^{\rm BPS}(\mathbf{r},a_{\rm MSA}(t)),$$

$$\Phi^{\rm MSA}(\mathbf{r},t)=\Phi^{\rm BPS}(\mathbf{r},a_{\rm MSA}(t)). \tag{1.1}$$

To test this approximation, we start with a configuration that is of this form at $t=0$; i.e., that satisfies

$$A_\mu(\mathbf{r},0)=A_\mu^{\rm BPS}(\mathbf{r},a_0),$$

$$\Phi(\mathbf{r},0)=\Phi^{\rm BPS}(\mathbf{r},a_0),$$

$$\dot{A}_\mu(\mathbf{r},0)=\dot{a}_0\frac{\partial A_\mu^{\rm BPS}(\mathbf{r},a_0)}{\partial a},$$

$$\dot{\Phi}(\mathbf{r},0)=\dot{a}_0\frac{\partial \Phi^{\rm BPS}(\mathbf{r},a_0)}{\partial a}, \tag{1.2}$$

with overdots denoting time derivatives. Since we expect the MSA to be most reliable when velocities are small, we take the initial cloud velocity $\dot{a}_0 \ll 1$. We also assume that the initial cloud size a_0 is much greater than the radius of the massive core.

These initial conditions determine a solution of the full field equations that can be compared with the MSA solution of Eq. (1.1). Although the spherical symmetry implied by the initial conditions simplifies the field equations somewhat, one is still left with a large number of coupled differential equations. However, the fact that the departures from the MSA are expected to occur primarily outside the massive core leads to a further simplification that reduces the problem to a single second-order equation. Analysis of this equation leads to a semi-quantitative understanding of the breakdown of the MSA. To test these ideas in detail, however, numerical methods are required.

In Sec. II we review the SO(5) theory in detail and describe the moduli space of BPS solutions. In Sec. III we set up the initial value problem that we will be considering. Here we analyze the field equations and obtain predictions for the expected departures from the MSA solution. In Sec. IV we describe the numerical solution of the field equations, and compare it with our expectations. In Sec. V we review our results and discuss their implications for the use of the MSA.

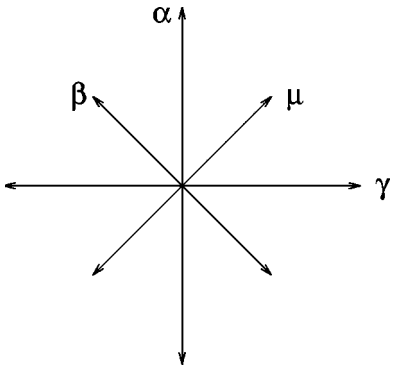

FIG. 1. The root diagram of SO(5).

II. SO(5) MONOPOLES

The generators of SO(5) may be chosen to be two commuting operators H_1 and H_2 that generate the Cartan subalgebra, together with eight raising and lowering operators $E_{\boldsymbol{\nu}_j}$, where the $\boldsymbol{\nu}_j$ are the roots shown in Fig. 1. (We fix the normalization of the gauge coupling by taking the long roots to be of unit length.) The vacuum expectation value of the adjoint Higgs field can always be chosen to lie in the Cartan subalgebra, and hence to be of the form $\Phi_\infty = h_1 H_1 + h_2 H_2 \equiv \mathbf{h}\cdot\mathbf{H}$. Furthermore, $\mathbf{h}$ can always be chosen so that $\mathbf{h}\cdot\boldsymbol{\beta}$ and $\mathbf{h}\cdot\boldsymbol{\gamma}$ are both positive. The two species of fundamental monopoles are then associated with the roots $\boldsymbol{\beta}$ and $\boldsymbol{\gamma}$ and have masses

$$M_{\boldsymbol{\beta}} = \frac{4\pi}{e}\frac{\mathbf{h}\cdot\boldsymbol{\beta}}{\boldsymbol{\beta}^2} = \frac{8\pi}{e}\mathbf{h}\cdot\boldsymbol{\beta}, \quad M_{\boldsymbol{\gamma}} = \frac{4\pi}{e}\frac{\mathbf{h}\cdot\boldsymbol{\gamma}}{\boldsymbol{\gamma}^2} = \frac{4\pi}{e}\mathbf{h}\cdot\boldsymbol{\gamma}. \tag{2.1}$$

The corresponding electrically-charged elementary gauge bosons have masses

$$m_{\boldsymbol{\beta}} = e\mathbf{h}\cdot\boldsymbol{\beta}, \quad m_{\boldsymbol{\gamma}} = e\mathbf{h}\cdot\boldsymbol{\gamma}. \tag{2.2}$$

If $\mathbf{h}\cdot\boldsymbol{\beta}$ and $\mathbf{h}\cdot\boldsymbol{\gamma}$ are both nonzero, the unbroken gauge group is $\mathrm{U}(1)\times\mathrm{U}(1)$. If instead $\mathbf{h}$ is orthogonal to $\boldsymbol{\gamma}$, the symmetry is only broken to $\mathrm{SU}(2)\times\mathrm{U}(1)$, and the $\boldsymbol{\gamma}$-monopole mass, like $m_{\boldsymbol{\gamma}}$, vanishes; this is the case we wish to consider. For convenience, we will define $v = \mathbf{h}\cdot\boldsymbol{\alpha} = 2\mathbf{h}\cdot\boldsymbol{\beta}$.

Index theorems [10] show that there is an eight-dimensional moduli space of BPS solutions containing one massive $\boldsymbol{\beta}$- and one massless $\boldsymbol{\gamma}$-monopole. Three of the collective coordinates can be chosen to be the center-of-mass coordinates $\mathbf{X}$, while four others can be taken to be the angles α, β, γ, and χ that specify the global $\mathrm{SU}(2)\times\mathrm{U}(1)$ orientation of the solution. Variations of these seven variables are equivalent to the actions of symmetry transformations. The dependence of the solutions on the last collective coordinate, which we take to be the cloud parameter a, is less trivial.

To display this dependence, we need some notation. We assemble the generators into a triplet

$$t_1(\boldsymbol{\alpha}) = \frac{1}{\sqrt{2}}(E_{\boldsymbol{\alpha}} + E_{-\boldsymbol{\alpha}}),$$

$$t_2(\boldsymbol{\alpha}) = -\frac{i}{\sqrt{2}}(E_{\boldsymbol{\alpha}} - E_{-\boldsymbol{\alpha}}),$$

$$t_3(\boldsymbol{\alpha}) = \boldsymbol{\alpha}\cdot\mathbf{H}; \tag{2.3}$$

a second triplet $t_a(\boldsymbol{\gamma})$, defined by analogous expressions involving $\boldsymbol{\gamma}$; and a quartet assembled into a 2×2 matrix

$$M = \sqrt{2}\, i \begin{pmatrix} E_{\boldsymbol{\beta}} & -E_{-\boldsymbol{\mu}} \\ E_{\boldsymbol{\mu}} & E_{-\boldsymbol{\beta}} \end{pmatrix}. \tag{2.4}$$

The spacetime fields can then be written as

$$A_i = \mathbf{A}_i^{(1)}\cdot\mathbf{t}(\alpha) + \mathbf{A}_i^{(2)}\cdot\mathbf{t}(\gamma) + \mathrm{tr}\,\mathbf{A}_i^{(3)} M,$$

$$\Phi = \boldsymbol{\Phi}^{(1)}\cdot\mathbf{t}(\alpha) + \boldsymbol{\Phi}^{(2)}\cdot\mathbf{t}(\gamma) + \mathrm{tr}\,\boldsymbol{\Phi}^{(3)} M. \tag{2.5}$$

With the $\mathrm{SU}(2)\times\mathrm{U}(1)$ symmetry breaking that we are assuming, the asymptotic Higgs field lies in the subgroup generated by the $\mathbf{t}(\boldsymbol{\alpha})$. The field components labeled by superscripts 1, 2, and 3 transform as three singlets, a triplet, and a complex doublet, respectively, under the unbroken SU(2).

In Ref. [9] it was shown that there is a static solution of the form

$$A^a_{i(1)} = \epsilon_{aim}\hat{r}_m A(r), \quad \Phi^a_{(1)} = \hat{r}_a H(r),$$

$$A^a_{i(2)} = \epsilon_{aim}\hat{r}_m G(r), \quad \Phi^a_{(2)} = \hat{r}_a G(r),$$

$$A_{i(3)} = \tau_i F(r), \quad \Phi_{(3)} = -iIF(r). \tag{2.6}$$

Here

$$A(r) = \frac{v}{\sinh evr} - \frac{1}{er} \tag{2.7}$$

and

$$H(r) = v\coth evr - \frac{1}{er} \tag{2.8}$$

are the functions appearing in the SU(2) unit BPS monopole, while

$$F(r) = \frac{v}{\sqrt{8}\cosh(evr/2)} L(r,a)^{1/2} \tag{2.9}$$

and

$$G(r) = A(r)L(r,a), \tag{2.10}$$

with

$$L(r,a) = [1 + (r/a)\coth(evr/2)]^{-1}. \tag{2.11}$$

At the center of this solution is a massive core of radius $\sim 1/ev$. Surrounding this is a non-Abelian cloud region whose size is set by the parameter a, which can take on any positive real value. Inside the cloud, in the region $1/ev \ll r \ll a$, the non-Abelian vector potential $\mathbf{A}_i^{(2)}$ falls as $1/r$ and yields a Coulomb non-Abelian magnetic field. In the region $r \gg a$, the non-Abelian magnetic charge is canceled by the cloud, and $\mathbf{A}_i^{(2)}$ falls more rapidly, as $1/r^2$.

Given the explicit form of the solution, it is a straightforward matter to obtain the metric on the moduli space, and thus the moduli space Lagrangian [4]

$$L_{\rm MS}=\frac{1}{2}M_{\beta}\dot{\mathbf{X}}^2+\frac{8\pi^2}{M_{\beta}e^4}\dot{\chi}^2 + \frac{2\pi}{e^2}\left\{\frac{\dot{a}^2}{a}+a[\dot{\alpha}^2+\sin^2\alpha\,\dot{\beta}^2+(\dot{\gamma}+\cos\alpha\dot{\beta})^2]\right\}. \tag{2.12}$$

III. FIELD EQUATIONS AND ANALYTICAL PREDICTIONS

Our goal in this paper is to understand how well the solutions given by the MSA approximate the solutions of the full field equations. To simplify matters, we will restrict ourselves to solutions with vanishing linear momentum and $SU(2)\times U(1)$ charges. The Euler-Lagrange equations that follow from Eq. (2.12) then imply that the only time-dependent collective coordinate is a, given by

$$a_{\rm MSA}(t)\equiv k(t+\Delta)^2 \tag{3.1}$$

where k and Δ are constants. The associated kinetic energy is

$$E=\frac{2\pi}{e^2}\frac{\dot{a}^2}{a}=\frac{8\pi k}{e^2}. \tag{3.2}$$

The MSA approximation to the fields is obtained by substituting Eq. (3.1) into Eq. (1.1). We want to compare this with the solution of the full field equations. Because of the spherical symmetry of the static BPS solutions, our initial conditions imply that the solutions will be spherically symmetric for all t. Even with this taken into account, the most general ansatz for the fields would involve a large number of functions of r and t. However, we expect that the deviations from the MSA arise primarily from the dynamics of the massless fields, rather than from the massive fields that are confined to the monopole core. Furthermore, we expect these deviations to manifest themselves primarily at large distances. Let us therefore choose some radius $\bar{r}$ that is large compared to the monopole core radius, but much smaller than the initial cloud size; i.e., $1/ev \ll \bar{r} \ll a_0$. We will assume that the MSA gives a good approximation to the fields at $r \ll \bar{r}$ for all t. (We will see that our numerical results are consistent with this assumption.) We then only need to solve the field equations for $r>\bar{r}$, subject to the boundary condition that the solution match onto the MSA solution at $r=\bar{r}$.

This leads to considerable simplification. The massive SU(2) doublet fields $A_\mu^{(3)}$ and $\Phi^{(3)}$ fall exponentially outside the monopole core and can therefore, to a good approximation, be set equal to zero in the region $r>\bar{r}$. Once this is done, the singlet and triplet fields are decoupled from each other. Since the former are independent of a, we can concentrate on the latter.

Requiring spherical symmetry and positive parity implies that the triplet fields must be of the form

$$A_i^{a(2)}=\epsilon_{aim}\hat{r}_m[G(r,t)+K(r,t)],$$
$$A_0^{a(2)}=\hat{r}_a J(r,t),$$
$$\Phi^{a(2)}=\hat{r}_a[G(r,t)-K(r,t)]. \tag{3.3}$$

J can be set equal to zero by a time-dependent gauge transformation. The Euler-Lagrange equations of the theory then reduce to

$$-\ddot{G}+G''+\frac{2}{r}G'-\frac{2}{r^2}G-\frac{2e}{r}G(2G+K)-2e^2(G+K)G^2=0, \tag{3.4}$$

$$-\ddot{K}+K''+\frac{2}{r}K'-\frac{2}{r^2}K-\frac{2e}{r}K(2K+G)-2e^2(G+K)K^2=0, \tag{3.5}$$

where overdots and primes denote differentiation with respect to t and r, respectively, and exponentially small quantities have been ignored.

The initial conditions of Eq. (1.2) imply that both K and $\dot{K}$ vanish for all r at $t=0$. It then follows from Eq. (3.5) that K will continue to vanish for all time. (One can also verify that small deviations from $K=0$ do not produce growing perturbations.) Defining $g(r,t)=-erG(r,t)$, we can then write

$$-\ddot{g}+g''-\frac{2}{r^2}g(1-g)^2=0. \tag{3.6}$$

This has the static solution

$$g_{\rm MS}(r,a)=\frac{a}{r+a}, \tag{3.7}$$

which corresponds to the $r \gg 1/ev$ limit of the BPS solution [Eq. (2.10)]. Note that $g\approx 1$ far inside the cloud, while far from the cloud g tends to zero.

The initial conditions of Eq. (1.2) reduce to

$$g(r,t=0)=g_{\rm MS}(r,a_0),$$
$$\dot{g}(r,t=0)=\dot{a}_0\left.\frac{\partial g_{\rm MS}(r,a)}{\partial a}\right|_{a=a_0}=\frac{r\dot{a}_0}{(r+a_0)^2}. \tag{3.8}$$

In addition, we have the boundary condition

$$g(\bar{r},t)=g_{\rm MS}(\bar{r},a_{\rm MSA}(t))=\frac{a_{\rm MSA}(t)}{\bar{r}+a_{\rm MSA}(t)}. \tag{3.9}$$

The time dependence of this boundary condition implies that the total energy in the region $r>\bar{r}$ will not be conserved. Physically, this is to be expected. Although the total energy of the static solutions is independent of a, the division of this energy between the core and the cloud varies with cloud size. Hence, even within the MSA there will be energy flow across the surface $r=\bar{r}$.

We will find it necessary to use numerical methods to solve Eq. (3.6). We will describe these in the next section. Before doing so, let us consider what type of departures from the MSA we might expect. We can distinguish two different ways in which the MSA might be expected to fail. First, the solution may depart from the moduli space by the excitation of low-frequency modes; i.e., by radiation. In the present context, this can occur because the time-dependent fields implied by the MSA act as a source for non-Abelian radiation. To make this more precise, let us write $g(r,t)=g_{\rm MS}(r,a_{\rm MSA}(t))+\delta g(r,t)$. If $\delta g \ll g_{\rm MS}$, we can linearize Eq. (3.6) to obtain

$$\begin{aligned}-\ddot{\delta g}+\delta g''-\frac{2}{r^2}(1-g_{\rm MS})(1-3g_{\rm MS})\,\delta g&=\ddot{g}_{\rm MS}\\ &=-\frac{2\dot{a}_{\rm MSA}^2 r}{(r+a_{\rm MSA})^3}+\frac{\ddot{a}_{\rm MSA} r}{(r+a_{\rm MSA})^2}\\ &=\frac{e^2E}{4\pi}\frac{r(r-3a_{\rm MSA})}{(r+a_{\rm MSA})^3},\end{aligned} \tag{3.10}$$

where E is the cloud kinetic energy given by Eq. (3.2).

The right hand side of this equation is concentrated in the cloud region, $r\lesssim a$. (For this initial analysis of the problem we ignore the $1/r$ tail.) Hence, we can view $\ddot{g}_{\rm MS}$ as the source for a radiation field δg that propagates outward from the cloud at the speed of light. In principle, we could solve for δg in terms of this source by using Green's function methods. However, because of the presence of the terms involving $g_{\rm MS}$, we have not been able to obtain a closed form expression for the Green's function.

Nevertheless, we can still estimate the rate of radiation; i.e., the power P that passes through a sphere of some fixed radius $r\gg a_0$. From Eq. (3.10) we see that $\delta G=-\delta g/(er)$ is proportional to eE. Since the radiation energy density is quadratic in derivatives of δG, the power must be of the form

$$P\sim e^2E^2f(\dot{a})\sim E\frac{\dot{a}^2}{a}f(\dot{a}), \tag{3.11}$$

with dimensional arguments showing that f cannot depend on a. It is also easy to see that f cannot depend on e. Although further analysis would be required to determine the form of $f(\dot{a})$ at small $\dot{a}$, it is presumably of order unity when $\dot{a}$ is of order unity.

The MSA must certainly break down by the time that the integrated power becomes comparable to the total energy of the cloud. Comparing Eqs. (3.2) and (3.11) and noting that the bulk of the energy loss occurs at large $\dot{a}$, where f is of order unity, we see that this happens when $t\sim a/\dot{a}^2\sim k^{-1}$. This is also the time that Eq. (3.1) predicts a cloud velocity comparable to the speed of light, a second indication of the breakdown of the MSA.

Because of its finite speed of propagation, the radiation described above can have no effect on the behavior of the fields at large distances; i.e., at $r>t$. However, there is a second type of breakdown of the MSA that occurs in this region. The MSA assumes that the system can be well described by a small number of time-dependent collective coordinates. This assumption can only be valid if retardation effects can be ignored, so that the system effectively reacts as a single unit to changes in the collective coordinates. This should be true within the cloud region as long as the characteristic time $a/\dot{a}$ is much greater than a; i.e., as long as the cloud velocity is much less than the speed of light. However, no matter how small $\dot{a}$ may be, we should expect departures from the MSA at distances $r\gg a/\dot{a}$.

We can examine this in more detail by using a large-distance expansion to solve Eq. (3.6). Let

$$g(r,t)=\sum_{n=1}^{\infty}\frac{C_n(t)}{r^n}. \tag{3.12}$$

Substituting this expansion into Eq. (3.6) gives a series of equations for the $C_n(t)$. The first two of these require that $\ddot{C}_1=\ddot{C}_2=0$. Integrating these with the initial conditions implied by Eq. (3.8) gives

$$\begin{aligned}C_1&=a_0+\dot{a}_0t,\\ C_2&=-a_0^2-2a_0\dot{a}_0t.\end{aligned} \tag{3.13}$$

Hence,

$$g(r,t)\approx g_{\rm MS}(r,a_0+\dot{a}_0t). \tag{3.14}$$

In other words, the large-distance fields are close to the moduli space of BPS solutions, but with a cloud size that grows at the initial velocity $\dot{a}_0$ rather than at the accelerating velocity predicted by the MSA.

IV. NUMERICAL RESULTS

We now turn to our numerical results. As explained in the previous section, we assume that the MSA is valid within a region of radius $\bar{r} \gg 1/ev$, and so only need to obtain a numerical solution for the region $r > \bar{r}$. The field equations then reduce to the single equation (3.6), which is to be solved subject to the initial conditions of Eq. (3.8) and the boundary condition of Eq. (3.9). To fix the initial conditions we must specify the initial cloud size, a_0, and the initial cloud velocity, $\dot{a}_0$. Because the cloud size sets the characteristic length scale for the spatial variations of the field, discretization errors will be reduced if $a_0 \gg \bar{r}$; for our solutions we take $a_0 = 50\bar{r}$. (The actual numerical value has no direct physical meaning, since our approximations effectively set $1/ev$, the only other physical length scale, equal to zero.) In order that we initially be in a regime where the MSA can be expected to be valid, $\dot{a}_0$ should be nonrelativistic; we choose $\dot{a}_0 = 0.01$. The parameters in Eq. (3.1) are then $k = 2.5 \times 10^{-5} a_0^{-1}$ and $\Delta = 200 a_0$.

We expect the MSA to break down at roughly the time that $\dot{a}_{\rm MSA}$ becomes of order unity; i.e., at $t \sim t_{\rm crit}$, where

$$t_{\rm crit} = \frac{1}{2k} = 2 \times 10^4 a_0 . \tag{4.1}$$

According to Eq. (3.1), $a_{\rm MSA}$ would then be $\sim 1/(4k) = 10^4 a_0$. Hence, to see the breakdown of the MSA we must follow the evolution of the system until the cloud has grown by several orders of magnitude. In order to make the computational load more manageable, we proceed as follows. Starting at $t = 0$, we numerically evolve the system over the range $\bar{r} < r < r_{\rm max}$, where $r_{\rm max} = 1000 a_0$. At $r = \bar{r}$, we require that g match onto the MSA solution. To fix the behavior at the other end of the interval, we use an expansion such as that given in Eq. (3.12) to obtain an analytic approximation to g for $r_{\rm max} < r < \infty$. We then require that the numerical solution match onto this analytic approximation at $r = r_{\rm max}$. As time goes on and the cloud expands, the spatial range of the numerical integration must be enlarged. To do this, we define a position $r_{1/2}(t)$ by the condition $g(r_{1/2}, t) = 0.5$. When $r_{1/2}$ grows to twice its original size, we replace $r_{\rm max}$ by $r'_{\rm max} = 2 r_{\rm max}$ and at the same time double the step sizes in our integrations. The new initial data is given for $\bar{r} < r < r_{\rm max}$ by the previous numerical results and for $r_{\rm max} < r < r'_{\rm max}$ by the large-distance analytic approximation. We continue in this fashion, doubling the interval and step sizes as required.

In Fig. 2 we show our results for $g(r)$ at six different times. For comparison, in each case we also show the predictions of the MSA. (Note that the distance scale changes from one panel to the next.) For the two earliest times, $t = 101 a_0$ and $t = 1030 a_0$, the MSA is clearly a good approximation to the exact solution. The only noticeable departure from the MSA appears to be due to the retardation effects at large distance; indeed, note the sharp bend in the data at $r = t$ that is visible at $t = 1030 a_0$ and all later times. The third time shown is approximately $t_{\rm crit}/2$. At this point the departures from the MSA are beginning to be significant, although the MSA still gives a fairly good qualitative picture. The times in the last three panels are all much greater than $t_{\rm crit}$. In these we see the numerical solution departing from the MSA and evolving toward a step-like profile in which g falls from 1 to 0 in a short interval near $r = t$. This step is essentially the radiation transformed into a sharp wavefront moving outward at the speed of light; it arises because the cloud that is the source of the radiation is now itself expanding at the speed of light. Although the step appears to be becoming narrower with increasing t, this is due to the change in distance scale from one panel to the next. Indeed, we see from Eq. (3.6) that far from the origin g is a function only of $r - t$, so that both the shape and the width of the step are constant at large time.

Despite this clear breakdown of the MSA at large distances, we find that it remains a good approximation to the data at shorter distances. To illustrate this, in Fig. 3 we plot the fractional deviation of g from the MSA prediction as a function of r/t for the times corresponding to the last three panels of Fig. 2. For any fixed $r/t < 1$ this fractional deviation decreases with time.

Another way to measure the deviation from the MSA is to define an r-dependent cloud parameter $a(r,t)$ by substituting the actual $g(r,t)$ into Eq. (3.7). In other words,

$$a(r,t) = \frac{r g(r,t)}{1 - g(r,t)} . \tag{4.2}$$

If the MSA were exact, $a(r,t)$ would be independent of r and equal to $a_{\rm MSA}(t)$. In Fig. 4 we plot $a(r,t)$ for several times ranging from $40 a_0$ to $80 a_0$. At all these times $a(r,t)$ is relatively flat near the origin, gradually falls, and then becomes approximately constant for $r > t$. The increase in the actual value in the latter region is very close to being linear in time, as predicted by Eq. (3.14).

We show the corresponding data for some larger times in Fig. 5, although with a rescaling of axes to allow easier comparisons between the data at the four different times. Again we see that $a(r,t)$ is roughly constant at smaller r, varying by no more than 10% for $r < t/4$.

V. CONCLUDING REMARKS

In this paper we have investigated the reliability of the MSA when applied to BPS monopoles in a theory with an unbroken non-Abelian symmetry. Whenever there are massless particles, the existence of non-BPS states arbitrarily close in energy to the BPS solutions raises the possibility that, no matter how small the kinetic energy, a time-dependent solution will deviate from the moduli space of static solutions to a sufficient extent to invalidate the MSA.

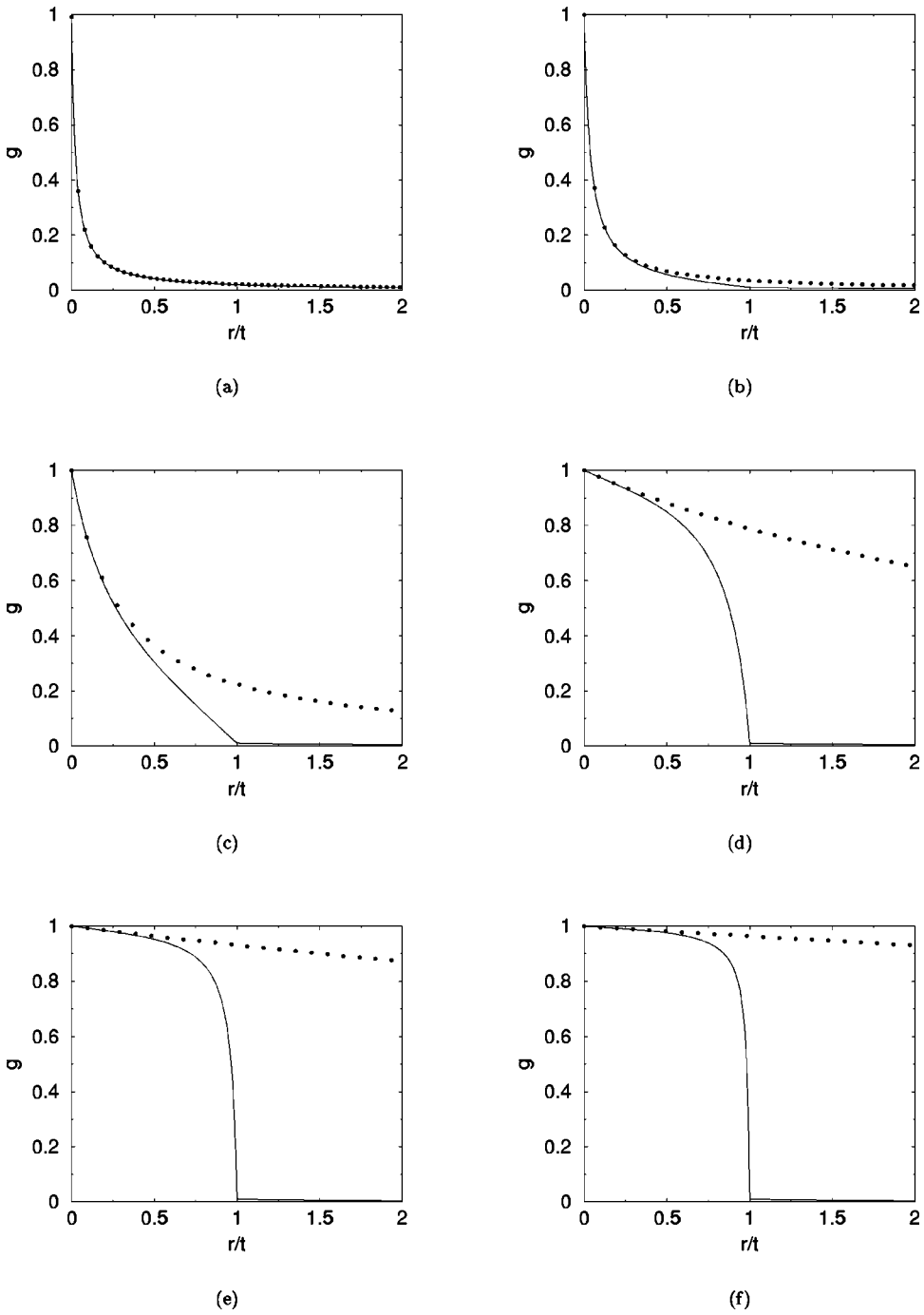

FIG. 2. Plots of the numerical solution (solid line) and MSA approximation (dotted line) for $g(r,t)$ at various times. Note that the distance scale varies from panel to panel. The panels correspond to (a) $t=101a_0$, (b) $t=1030a_0$, (c) $t=1.11\times10^4a_0$, (d) $t=1.49\times10^5a_0$, (e) $t=5.45\times10^5a_0$, and (f) $t=1.07\times10^6a_0$.

For the case of Abelian massless fields, previous investigations have shown that the radiation processes that might give rise to such departures fall as a power of velocity and so can be neglected to leading approximation at low energy. We have found that this is not the case when the massless fields are non-Abelian.

The time-dependent fields in the cloud region surrounding the massive monopoles act as sources for non-Abelian radiation. As in the Abelian case, radiation is suppressed at low velocities; in particular, the power radiated is proportional to the square of the cloud kinetic energy. The crucial difference lies in the duration of the radiation. The Abelian radiation in a multimonopole system falls off as the massive monopoles recede from each other. By contrast, the non-Abelian radiation in our system continues unabated as the cloud expands. The net effect is that the field profiles depart sharply from the MSA prediction by the time the cloud velocity approaches unity.

Despite this, we do not find a complete breakdown of the MSA. It remains quite reliable as long as the cloud velocity is small. Even when the cloud has become relativistic, the MSA gives a good description of the fields well inside the cloud (say for $r\lesssim t/4$). If the massive monopoles within the cloud remain nonrelativistic, they will always be in the region where the MSA is valid. Hence, one should be able to use the MSA to describe both the motion of the massive

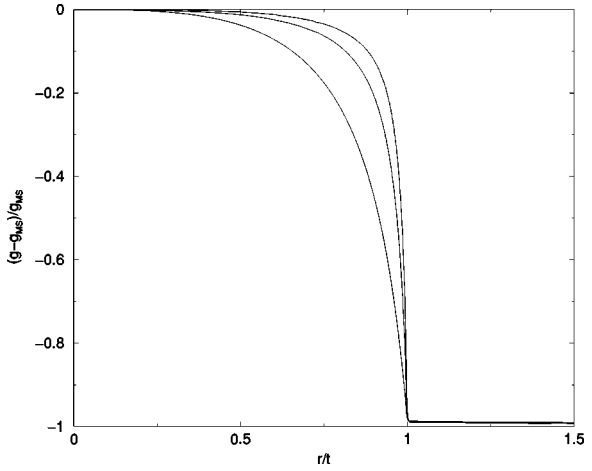

FIG. 3. Fractional deviation of $g(r)$ from the MSA prediction. From inner to outer, the curves correspond to $t=1.49\times10^5a_0$, 5.45×10^5a_0, and 1.07×10^6a_0. Note that the distance scale increases with time.

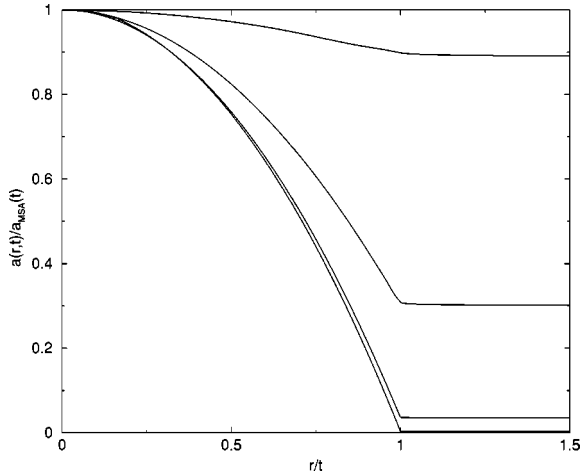

FIG. 5. Plot of $a(r,t)$. Reading from the top, the curves correspond to $t=101a_0$, 1.03×10^3a_0, 1.1×10^4a_0, and 1.49×10^5a_0. Note that the distance scale increases with time.

monopoles and the transfer of energy between the massive and massless monopoles. Furthermore, the cloud does survive as a clearly identifiable object in the classical solution, although the smoothly varying profile of the static BPS solution is transformed into a relativistic wavefront. In a sense, the modifications to the MSA that we have found are the minimal ones consistent with the relativistic bound on velocity.

Although we have focussed on the case where there is a strictly massless monopole, we should make a few remarks on the situation when one of the monopoles is massive but much lighter than all the others. For the analogue of our SO(5) example Eq. (3.2) is replaced by

$$E=\frac{2\pi}{e^2r_0}\left(\frac{r+r_0}{r}\right)\dot{r}^2=\frac{1}{2}\mu\left(\frac{r+r_0}{r}\right)\dot{r}^2, \tag{5.1}$$

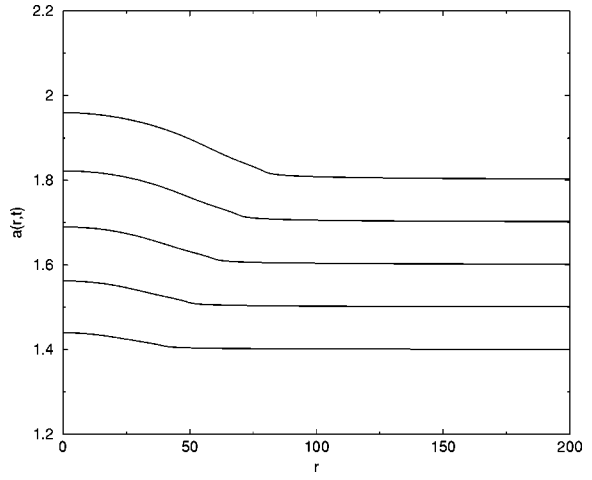

FIG. 4. Plot of $a(r,t)$. Reading from the bottom, the curves correspond to $t=40a_0$, $50a_0$, $60a_0$, $70a_0$, and $80a_0$. The distances are given in units of a_0.

where r is the separation of the two monopoles, μ is the reduced mass of the monopole pair, and $r_0\equiv4\pi/e^2\mu$ gives the size of the lighter monopole core when the monopoles are well separated.

When $r\lesssim r_0$, the two monopoles are overlapping, with the core of the lighter monopole enclosing the heavier monopole. This core is then much smaller than its natural size and has a radius approximately equal to r. In this regime $\dot{r}$ grows linearly with time, as in the massless case, and only tends to a constant value $\sqrt{2E/\mu}$ after the two cores separate. If $E\ll\mu$, the two monopoles are always nonrelativistic, and the MSA is reliable. If instead $E\gtrsim\mu$, a breakdown of the MSA, similar to that which we have seen in this paper, occurs while the two monopoles are still overlapping. We would expect this to lead to a deformation of the core profile of the lighter monopole so that initially, like the cloud in the massless case, it resembles a spherical wavefront expanding at the speed of light. However, when the core radius becomes of order r_0, this wavefront presumably splits into a shell of radiation that continues to expand and a massive core that is left behind. The heavier monopole will eventually separate from this core, but not from the outgoing shell of radiation.

For this two-body system the validity of the MSA is assured if the initial relative velocity is small, since the final configuration is nonrelativistic if the initial one is. This need not be true in a three-body system. An example occurs in an SU(3) theory broken to U(1)×U(1) with one of the fundamental monopoles being much lighter than the other. Consider a configuration containing one of the light and two of the heavy monopoles. Because there can be a net transfer of energy from the heavy to the light monopoles, it is possible for the light monopole to initially have $v\ll1$ but to emerge with a relativistic final velocity. As a result, the MSA fails at large times, as was first pointed out by Irwin [11].

Finally, let us consider what happens as we move toward the strong coupling (large e) limit, where the duality conjecture leads us to expect the solitons and elementary particles to exchange roles. Even without taking into account the quantum corrections to the classical field profiles, we can see

how the classical soliton picture is lost. For the massive monopoles this is signalled by the fact that the core radius $\sim 1/(e^2M)$ becomes less than the Compton wavelength, so that a nonrelativistic monopole cannot be sufficiently localized for its solitonic properties to be directly observable. For the massless monopoles, the transition can be seen by focussing on the two phases in the evolution of the massless cloud. For a time interval of order $t_{\rm crit} \sim 1/(e^2E)$ the cloud behaves like a slowly expanding soliton, as predicted by the MSA. Beyond this time, it resembles a wavefront expanding at the speed of light. In the strong coupling limit, $t_{\rm crit}E$ is much less than unity. The uncertainty principle then implies that the period when the massless monopoles behave like nonrelativistic solitons is unobservably short; instead, they will always appear as a wavefront of radiation moving at the speed of light. In retrospect, this makes it seem quite natural that, even in the weak-coupling regime, the cloud cannot be kept nonrelativistic.

ACKNOWLEDGMENTS

This work was supported in part by the U.S. Department of Energy.

[1] N.S. Manton, Phys. Lett. **110B**, 54 (1982).
[2] E.B. Bogomolny, Yad. Fiz. **24**, 861 (1976) [Sov. J. Nucl. Phys. **24**, 449 (1976)].
[3] M.K. Prasad and C.M. Sommerfield, Phys. Rev. Lett. **35**, 760 (1975).
[4] K. Lee, E.J. Weinberg, and P. Yi, Phys. Rev. D **54**, 6351 (1996).
[5] X. Chen and E.J. Weinberg, Phys. Rev. D **64**, 065010 (2001).
[6] N.S. Manton and T.M. Samols, Phys. Lett. B **215**, 559 (1988).
[7] D. Stuart, Commun. Math. Phys. **166**, 149 (1994).
[8] E.J. Weinberg, Nucl. Phys. **B167**, 500 (1980).
[9] E.J. Weinberg, Phys. Lett. **119B**, 151 (1982).
[10] E.J. Weinberg, Nucl. Phys. **B203**, 445 (1982).
[11] P. Irwin, hep-th/0004054.